Research Article

Combustion Assisted Synthesis of CuO Nanoparticles and Structure-Property Evaluation in nano-CuO Polymer Composites

Gopinath Prasanth and Gattumane Motappa Madhu*
Department of Chemical Engineering, M. S. Ramaiah Institute of Technology, MSR Nagar, Bengaluru, Karnataka, India

Nagaraju Kottam
Department of Chemistry, M. S. Ramaiah Institute of Technology, MSR Nagar, Bengaluru, Karnataka, India

* Corresponding author. E-mail: gmmadhu@msrit.edu DOI: 10.14416/j.asep.2023.11.009
Received: 16 August 2023; Revised: 8 September 2023; Accepted: 5 October 2023; Published online: 22 November 2023

Abstract
Metal oxide-based nanoparticle as a filler in epoxy polymer composites has diverse applications in various industries, including adhesives, automobiles, aerospace, wind energy, and civil engineering. However, these composites must fulfill essential properties encompassing chemical, curing, optical, and thermal attributes. This study focuses on enhancing epoxy polymer by integrating copper oxide (CuO) nanoparticles synthesized through solution combustion. Varied CuO loadings (0.5–2.5 wt.%) were impregnated into the epoxy, critically impacting the structural attributes of the resulting nano-CuO polymer composites. Various material characterization techniques were employed to study the synthesized materials' morphology, elemental composition, phase formation, identification of the presence of functional groups, thermal stability, and optical properties. SEM images show the presence of spherical particles with porous structures. EDX confirmed the presence of Cu and O elements, while the XRD pattern showed the formation of CuO with an average crystallite size of 46 nm. FTIR confirms the presence of O-H, C-H, and C=C functional groups. TGA showed thermal stability and revealed minimal mass loss below 250 °C for nano-CuO polymer composites and minimal mass loss occurred for CuO nanoparticles at 900 °C. Photoluminescence exhibited redshifted luminescence spectra. The study suggests improved qualities due to CuO nanoparticle integration into epoxy. CuO loading crucially influences nano-CuO polymer composite properties, rendering them ideal for high-temperature applications, supported by remarkable thermal stability evidenced by substantial residual mass in TGA.

Keywords: CuO nanoparticles, Epoxy-resin, Material characterization, Polymer-composites, Structure-property analysis

1 Introduction

The combustion synthesis method is most commonly used for producing homogeneous, finely dispersed crystalline oxides, which are uniformly sized, characterized metals and alloys [1]. This method does not require intermediary preparation processes, which are quick, simple, and take less time. The combustion route is employed for the synthesis of several kinds of metal-based materials, including nitrides, metals perovskites, oxides, carbides, and alloys used in diverse applications [2]. Among the various combustion processes, the solution combustion method is unique, particularly for the synthesis of metal oxide nanoparticles, and it can be employed for obtaining the desired qualities of oxides for a variety of applications by varying the composition of metals during the synthesis. The solution combustion route is used for synthesizing homogeneous products with low ignition temperatures than self-propagating high-temperature synthesis. Organic molecules such as glycine and citric acid with functional groups are used as fuels, and metal

nitrates as oxidizers in the solution combustion process. When the mixture of fuel and metal nitrates is heated, non-agglomerated solid particles are produced as a result of the highly exothermic combustion reaction between the oxidizer and fuel, which also produces significant amounts of gaseous products. The shape and particle size of produced nanoparticles are often significantly affected by the type and amount of fuel present in a reaction mixture. In some circumstances, the quantity and kind of fuel may promote phase change and the development of metastable phases [3], [4]. As a type of significant inorganic substance, copper oxide (CuO) nanoparticles are frequently used in the fields of catalysis, superconductors, and ceramics. Thus, it can be utilized as a catalyst, and electrode-active material for processes such as the oxidation of carbon monoxide, hydrocarbons, and phenol in supercritical water and the degradation of nitrous oxide with ammonia [4]–[10]. The "solution combustion method of nanoparticle synthesis" is a chemical synthesis technique used to synthesize nanoparticles, which are extremely small particles with dimensions typically in the range of 1–100 nm. This method involves the rapid and exothermic reaction between metal salts or metal-containing compounds and a suitable fuel, often an organic compound. The reaction takes place within a liquid medium, usually a solvent, and results in the formation of nanoparticles suspended within the solution [11], [12].

Fillers of various sizes are commonly employed as reinforcement for polymers to improve their properties, overcoming some of the restrictions of polymers and expanding their uses. Traditional polymer composites have been replaced by an innovative substitute using nanoscale fillers to enhance polymer's mechanical, physical, and chemical properties. The three main categories of nanofillers include two-dimensional (2D) layered materials like silicate and graphene and one-dimensional (1D) materials like carbon nanofibers and nanotubes. Fibrous and zero-dimensional (0D) materials like quantum dots and spherical silica [13]–[17]. Nanometal oxide polymer composites contain nanoscale metal particles within a matrix of conventional polymer material. When metal nanoparticles are embedded in polymers, the properties, including toughness, mechanical strength, and thermal conductivity or electrical, are significantly improve [18]. Typically, less than 5 wt.% of metal nanoparticles are embedded within the polymer matrix due to their high efficiency in influencing the properties of the polymer composites [19]–[23].

Metal nanoparticles incorporated into polymer composites will provide them with more unique qualities for use in a variety of applications. Because of the peculiar optical properties of metal nanoparticles like CuO, which depend on both their size and shape, these nanoparticles have potential uses as heterogeneous catalysts, imaging agents, and drug delivery systems, among other things. In view of this, current research has focused on synthesizing metal-polymer nanocomposite using CuO nanoparticles for usage as effective reinforcement polymers and drug carriers. In this context, the present work is aimed at synthesizing nano CuO and epoxy composite materials by varying amounts of synthesized CuO nanoparticles. Various techniques such as Scanning Electron Microscope (SEM), X-ray diffraction (XRD), Fourier-transform infrared spectroscopy (FTIR), and Energy dispersive X-ray (EDX) were used to characterize the synthesized nanomaterial and composites. Experiments have been carried out to determine whether CuO nanoparticle loading influences polymer curing time, thermal characteristics, and optical properties. These properties are crucial for such nanocomposites when they are used as reinforcing materials.

CuO nanoparticles and nano CuO polymer composites are highly versatile materials with significant applications in aerospace applications [24]. They possess unique properties, such as size-dependent optical and catalytic characteristics, making them essential in modern technology [24]. To maximize their potential in aerospace, a range of analytical techniques is essential for characterization, including SEM and EDX for surface morphology and elemental composition, XRD for crystal structures, FTIR for functional groups, TGA for thermal stability, and PL spectroscopy for optical properties [25]. These thorough characterizations enable customization to meet aerospace demands. In the aerospace sector, these materials excel in extreme conditions, seamlessly integrating into critical components like engine parts, heat shields, and structural elements [26]. They enhance safety and durability while also serving as efficient reinforcement polymers, improving the thermal properties of aircraft construction materials. This results in reduced weight, enhanced fuel efficiency, and improved overall aerospace

system performance [24].

CuO nanoparticle content in the synthesis of CuO nanoparticles and nano-CuO epoxy composite materials intends to improve the properties of the composite, and broaden its applications across various fields. The loading's influence of CuO nanoparticle on the nanocomposite's performance parameters holds paramount significance [27]. These parameters show that polymer curing kinetics, thermal properties, and optical behaviors, are instrumental in defining the composite's suitability for specific applications. The incorporation of nanofillers into polymer matrices offers a promising strategy to enhance resistance against chemical degradation and environmental challenges. This advancement is particularly valuable for applications exposed to harsh chemicals and extreme conditions, as observed in industrial and outdoor settings. This approach holds substantial potential for addressing durability concerns in demanding operational environments [28]–[30].

The CuO nanoparticles have gained significant attention due to their unique properties, which make them suitable for a wide range of applications across various fields. The properties of copper oxide nanoparticles include their size-dependent optical, electrical, magnetic, and catalytic characteristics. Here are some key applications based on these properties, like catalysis, coatings, and nanocomposites. Epoxy polymers are known for their biocompatibility, stability, and tunable properties, making them suitable candidates for designing drug delivery systems. Using epoxy polymers for drug delivery is an emerging area of research with potential applications in the field of pharmaceuticals [31].

2 Materials and Methods

2.1 *Materials*

The precursor salt of copper nitrate trihydrate ($Cu(NO_3)_2.3HO$, ≥ 90 %), and glycine (CH_2NH_2COOH) were obtained from Sigma-Aldrich. The Lapox L-12 epoxy resin and Lapox K-6 hardener were used as received. Deionized water was used for metal precursor solutions preparation.

2.2 *Synthesis of CuO nanoparticles*

The CuO nanoparticles were produced by the solution combustion method. Glycine was mixed with the copper (II) nitrate trihydrate precursor salt as a fuel to enhance combustion. The fuel-to-nitrate ratio (F/N) was maintained at 0.3, for which 19.372 g of copper nitrate trihydrate, and 1.8 g of glycine were dissolved in 125 mL of deionized water. The reaction mixture was continuously stirred on a hot plate. As the heating continued, gases such as carbon dioxide, water vapor, and nitrogen dioxide (it had a reddish brown color and a strong odor) were liberated, which led to the development of a gel. Within a few minutes of the gel formation, the reaction was completed by self-ignition combustion, yielding an extremely fine, porous powder. Then, the final product was dried at 80 °C overnight and then calcined at 600 °C for 3 h. The solution combustion reaction for the synthesis of CuO nanoparticles is shown below in Equation (1):

$$13Cu(NO_3)_2{\cdot}3H_2O + 2CH_2\ NH_2COOH \rightarrow 13CuO + 4CO_2 + 44H_2O + 28NO_2 \quad (1)$$

2.3 *Preparation of nano CuO polymer-epoxy composite*

A known quantity of epoxy was taken, and after being sonicated for 45 min in a 200 W ultrasonicator, the temperature of the epoxy started to increase up to 60 °C. Once it was cooled to room temperature, epoxy and hardener were mixed and casted onto a mold. The mixture was dried at room temperature for 24 h. To obtain pristine epoxy, 90% resin and 10% hardener by volume were mixed together. The same procedure was carried out to obtain polymer composites doped with different proportions of CuO. Different weight percentages (wt.%) of CuO, such as 0.5, 1.0, 1.5, 2.0, and 2.5 wt.% were prepared. The epoxy and nano-CuO polymer epoxy composites were obtained after drying. Digital Vernier calipers were used to measure thickness; the average thickness of the pristine epoxy and epoxy composite was found to be around 3 mm.

2.4 *Material characterization techniques*

The elemental composition and morphology of the CuO nanoparticles and nano-CuO polymer composites were carried out using a Hitachi S-3400 SEM with energy-dispersive X-ray spectroscopy (EDX) employed with INCA EDS detector. XRD measurements were performed using an X-ray diffractometer with a tube

voltage and current of 40 kV and 40 mA. The Bruker D8 ADVANCE (Karlsruhe, Germany) was used to obtain the X-ray diffraction data using a Cu Kα (λ = 1.5406 Å) and a Ni filter to produce X-rays. The data was gathered in the 2θ ranging from 10–90° with a step size of 0.02°. The spectral data recorded in % transmittance with a bandwidth of 5 nm were acquired using the ALPHA FTIR (Bruker) in the range of 4000–500 cm^{-1} in ECO-ATR transmittance mode. A total number of 64 scans were performed in FTIR analysis with a resolution of 4 cm^{-1}. Thermal properties were analyzed using a Thermal Analyzer-Nitrogen STA 449 F5 Jupiter, N_2 gas is used as sweeping gas in a SiC furnace. The mass loss data was acquired in the temperature range of 30–900 ℃ for CuO nanoparticles with a heating rate of 10 ℃/min, and the gas flow rates were maintained at 20 mL/min for Gas Flow (protective) and 50 mL/min for Gas Flow (purge2). For the TGA experiments, an empty Al_2O_3 crucible was used for the reference and Al_2O_3 crucible filled with the sample was used for the CuO nanoparticle. The same parameters were used for the nano-CuO epoxy polymer composites except for the heating temperature; in this case, TGA was carried out from 30–250 ℃. The choice of this shorted temperature is in line with the reported value and beyond this value, the polymer starts to degrade. The F2700 fluorescence spectrometer is a used tool for analyzing the fluorescence characteristics of CuO and Epoxy composites.

3 Results and Discussion

3.1 *FE-SEM and EDX analysis*

From SEM images it can be observed that the CuO nanoparticles appear to be broadly spherical in shape similar to earlier works reported. Figure 1 shows the pure CuO nanoparticles that are spherical, porous, and agglomerated. CuO nanoparticles have a size that ranges from 35.3–72.4 nm. The large surface energy and huge surface area of the nanoparticles cause the agglomeration of the particles. Large Van der Waals surface charges result in agglomeration under nano size. Figure 2 shows the SEM images of (a) Pristine epoxy and epoxy-CuO polymer composites with an amount of CuO (b) 0.5 wt.%, (c) 1.0 wt.%, (d) 1.5 wt.%, (e) 2.0 wt.%, and (f) 2.5 wt.%. From Figure 2 at lower concentrations, it was seen that the nanoparticles were

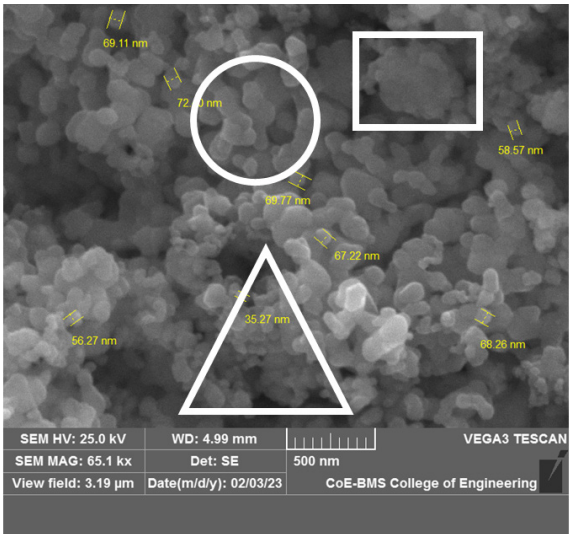

Figure 1: The scanning electron microscopy (SEM) images of copper oxide nanoparticles synthesized using the solution combustion method. The particles present within the square box are agglomerated, the particles with a sphere shape are shown using a circle, and particles depicting the porous structure are shown within the triangle.

evenly dispersed throughout the epoxy. The higher concentrations of the nanofiller led to agglomeration, and large masses are observed in some of the images. The degree of CuO nanoparticle aggregation increased with an increase in filler content. The homogenous dispersion of nanofillers in an epoxy polymer is one of the major obstacles to synthesizing polymer composites [32]–[36]. The polymer composite's thermal characteristics were subsequently impacted by the increased agglomeration. EDX spectrum shows four major peaks at around 0.3 keV for O element, and 0.85, 8.0, and 8.6 keV peaks belong to element Cu (Figure 3). Further, EDX was used to assess the potential impurities and provide information on the elemental composition of synthesized CuO nanoparticles, as shown in Figure 3. The elemental composition of CuO is presented in Table 1.

Table 1: The elemental composition of CuO nanoparticles that was measured using energy dispersive X-ray (EDX)

Element	Weight (%)	Atomic (%)
Cu	83.26	55.60
O	16.74	44.40

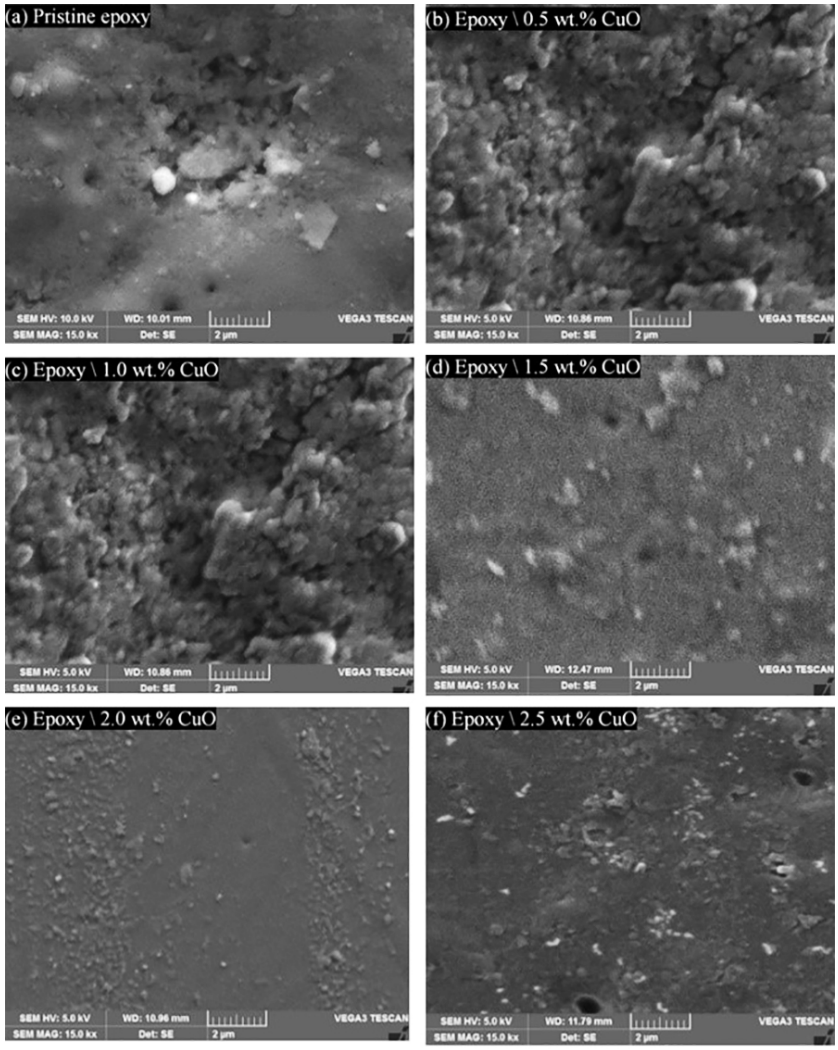

Figure 2: The scanning electron microscopy (SEM) micrographs of (a) Pristine epoxy and epoxy-CuO polymer composites with the amount of CuO (b) 0.5 wt. %, (c) 1.0 wt. %, (d) 1.5 wt. %, (e) 2.0 wt. %, and (f) 2.5 wt. %.

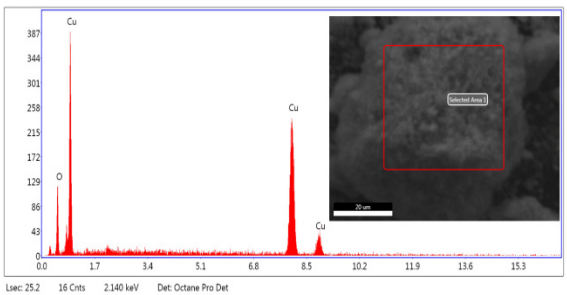

Figure 3: EDX plot for the support of the presence of Cu and O elements.

3.2 *Powder XRD of CuO and epoxy-CuO composites*

The XRD patterns of the CuO nanoparticles are presented in Figure 4, and these patterns show prominent peaks. The typical strong peaks in the XRD pattern of CuO can be found at angles of about $2\theta = 32.5, 35.5, 38.8, 48.5, 53.9, 58.1, 61.1, 66.2, 68.1,$ and $75.1°$, which correspond to the (110), (002), (111), (112), (202), (311), (022), (220) and (311), respectively crystal planes of the CuO crystal structure. The CuO sample was highly crystalline and matched with the CuO crystal structure JCPDS file JCPDS 48-1548.

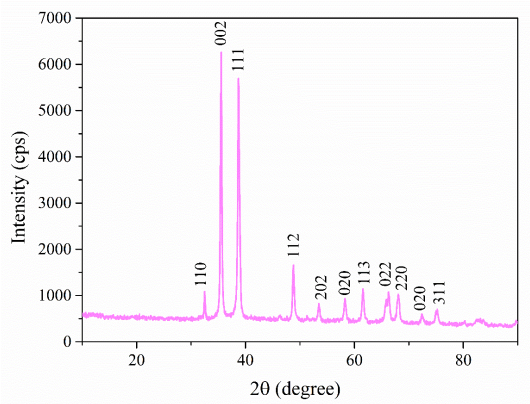

Figure 4: The powder X-ray diffraction (XRD) pattern of copper oxide nanoparticles synthesized using the solution combustion method with a lattice plane for each peak.

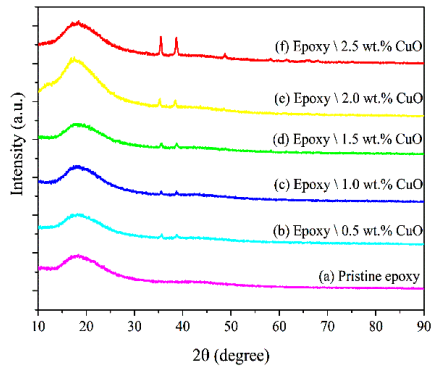

Figure 5: The powder x-ray diffraction (XRD) pattern of (a) pristine epoxy sample and nano-CuO polymer composites with an amount of CuO impregnation of (b) 0.5 wt.%, (c) 1.0 wt.%, (d) 1.5 wt.%, (e) 2.0 wt.% and (f) 2.5 wt.%.

The Scherrer equation, factoring FWHM, X-ray wavelength, and diffraction angle, this comprehensive approach reveals particle homogeneity and method reliability in nanomaterial characterization. CuO crystallite size was determined using the Scherrer equation that utilizes FWHM of peaks, analyzing diffraction peaks in XRD patterns that correlate with the atomic arrangement in crystals [37]. The broader peaks indicate more significant size variation.

The size of the crystallite (D) was calculated using Debye–Scherrer formula [38], using Equation (2).

$$D = 0.9\lambda/\beta cos\theta \quad (2)$$

where λ represents the wavelength of the X-ray source employed (0.15418 nm) corresponding to Cu K-alpha radiation. β is the full width at half maximum (FWHM) and θ is the angle of diffraction [37]. The calculated average crystallite size was determined to be 46 nm. This value is within the range of particle size measured using the SEM data. In addition, the crystallite size calculated in the present study closely matches the literature value of 20.7 nm [39].

The aggregated cluster in the composite polymer nano-CuO polymer ranges up to 500 nm. The level of saturation also rises when the CuO concentration increases from 0.5–2.5 % by weight in the nano-CuO polymer composite, minimizing the distance between CuO molecules between particles [40], [41].

The XRD patterns of polymer composite, containing CuO nanoparticles from 0.5–2.5 wt%, exhibited prominent, powerful peaks, which point to the degree of CuO addition into the epoxy matrix, as shown in Figure 5. The amount of CuO loading determines the strong peaks in the polymer composites. The XRD patterns exhibited an increase in peak intensity when the amount of CuO increased from 0.5–2.5 wt%, indicating an increase in crystallinity and the amount of CuO present in the polymer composites. The peak position did not change with the increase in CuO loading [4].

The XRD demonstrated epoxy's slightly amorphous nature and profile, shown in Figure 4 with 92% of crystallinity. Figure 5 shows the XRD patterns of nano-CuO polymer composites with different amounts of CuO from 0.5–2.5 wt.%. The crystalline character of epoxy is demonstrated by the peak of all the polymer composites showed at about 2θ = 18.5°, which corresponds to the epoxy (110) crystal plane. Few peaks around 35 and 50° were observed with the addition of CuO nanofillers. The intensity of these peaks increased with an increase in the amount of CuO nanoparticle impregnation [41].

3.3 *Fourier-transform infrared spectroscopy (FT-IR)*

The FTIR spectra of CuO and nano-CuO polymer composites are shown in Figures 6 and 7. CuO exhibited distinctive peaks in the FTIR spectrum between

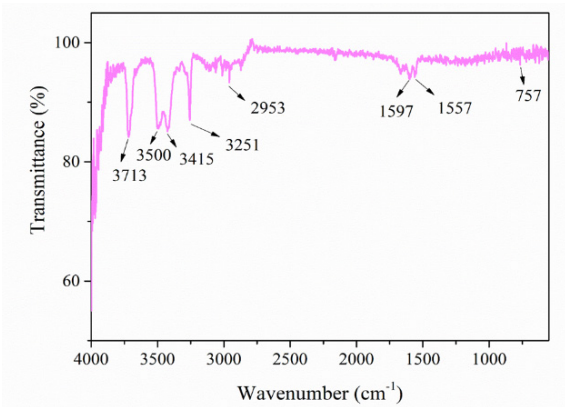

Figure 6: FTIR spectrum of CuO nanoparticles shows certain vibrational modes or functional groups.

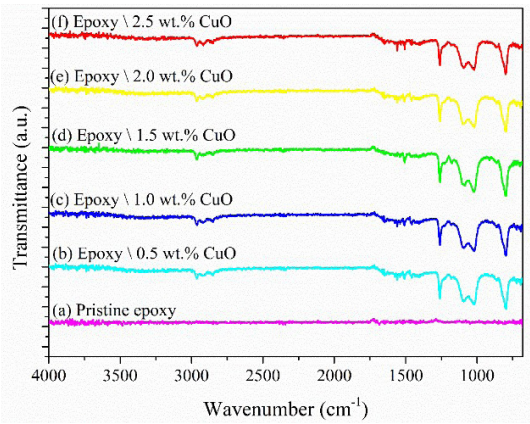

Figure 7: FTIR spectra of (a) Pristine epoxy and nano-CuO polymer composites with (b) 0.5 wt.%, (c) 1.0 wt.%, (d) 1.5 wt. %, (e) 2.0 wt. %, and (f) 2.5 wt.% of CuO nanoparticles loading.

4000 and 1200 cm^{-1}, which are associated with CuO stretching vibrations [42]. The peaks at 3500 cm^{-1} indicate the O-H stretching vibrations of the water adsorbed on the CuO surface. The peaks at 3415 cm^{-1} indicate the presence of surface hydroxyl groups. The peak at 3000–1300 cm^{-1} indicates the presence of a C-H group (Table 2). The FTIR spectrum showed peaks at around 1597 cm^{-1} indicating the presence of C=C groups [43]–[45].

The intensity of the CuO stretching vibration peak increases as the weight of CuO in the polymer composites rises from 0.5 to 2.5 wt.%. This indicates the peak's intensity is related to the amount of CuO present in the polymer composites. A peak of about

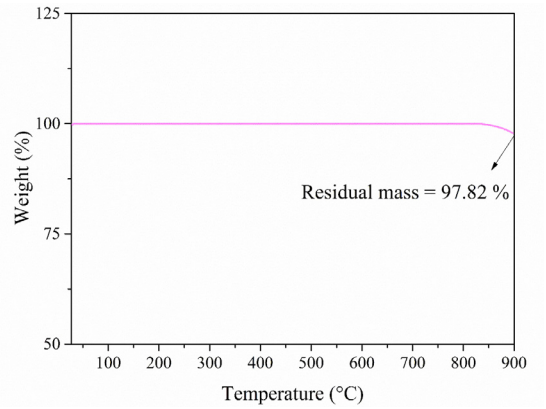

Figure 8: Thermogravimetric analysis of CuO nanoparticles, which shows the weight loss in percentage in terms of temperature.

1400–500 cm^{-1} indicates the presence of a C-O group. Figure 7 of FTIR spectra exhibited peaks at about 1300 cm^{-1} and 800 cm^{-1} are associated with the C-O stretching vibrations. This peak's intensity rises with an increase in the weight of CuO nanoparticles in the polymer composites [46]–[48].

Table 2: FTIR peaks and respective vibrational modes

Sample	Wavenumber (cm^{-1})	Functional Groups
CuO nanoparticles	3500	O-H stretching vibrations
	3415	Surface hydroxyl groups
	3000–1300	C-H group
	1597	C=C groups
Nano-CuO polymer composites	1400–500	Presence of a C-O group
	1300 and 800	C-O stretching vibrations

3.4 *Thermogravimetric Analysis (TGA)*

The TGA of CuO nanoparticles was tested at temperatures ranging from 30–900 °C. From Figure 8 the residual mass of CuO nanoparticles was found to be 97.82% at 900 °C, 2.18 % of the initial mass was lost at 900 °C for CuO nanoparticles during the decomposition process, and no mass loss at the end of 250 °C. The CuO nanoparticles are ideal for high-temperature applications because of their remarkable thermal stability, which is indicated by their large residual mass. CuO nanoparticle's exhibit exceptional thermal stability and structural integrity because of great surface area and crystallinity. CuO nanoparticles

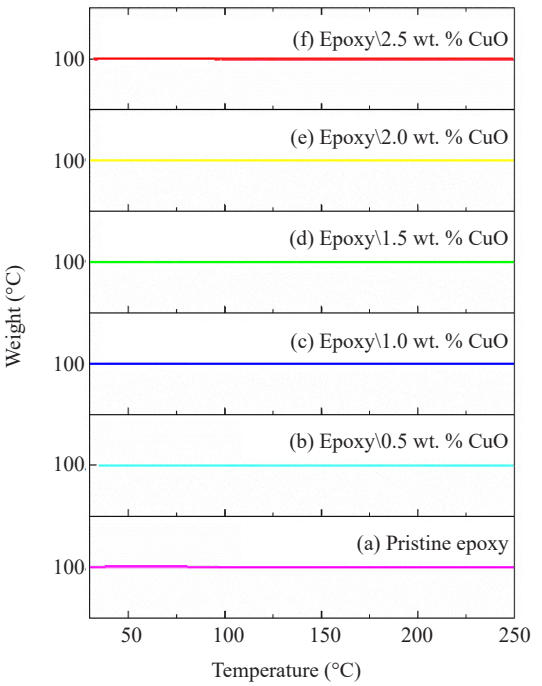

Figure 9: Thermogravimetric plots of (a) Pristine epoxy and nano-CuO polymer composites with (b) 0.5 wt.%, (c) 1.0 wt.%, (d) 1.5 wt.%, (e) 2.0 wt.% and (f) 2.5 wt. % of CuO nanoparticles impregnation for the temperature from room temperature (30 °C) to 250 °C.

crystallinity also shows that the substance maintains its structural integrity even at high temperatures [49].

For the nano-CuO polymer composites, the polymer composite samples with transition temperature values were measured at 250 °C. The degree of polymer chain mobility and the cross-linking density of an epoxy polymer directly impact the polymer's temperature [50]. The nano-CuO polymer composite's residual mass was found to be 99% at 250 °C for 0–1.0 wt% and 100% at 250 °C for 1.5–2.5 wt% of CuO loaded polymer composite. It has almost 99–100% of the residual mass for all CuO loadings (Figure 9 and Table 3). This shows that very minimal substance had broken down at this temperature. The existence of residual mass shows that the CuO nanoparticles had a major impact on the epoxy matrix's thermal stability. The excellent thermal stability of CuO nanoparticles, which can function as a thermal barrier and stop the degradation of the epoxy matrix, can be linked to the high residual mass [4].

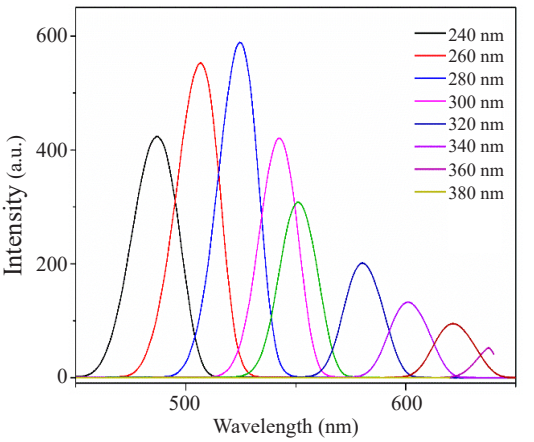

Figure 10: Luminescence spectra of CuO nanoparticles.

Table 3: The residual mass of CuO nanoparticles and CuO-impregnated epoxy polymer composites at 250 °C

Samples	CuO Weight (%)	Residual Mass at 250 °C (%)
CuO	-	100.00
(a) Pristine epoxy	0.0	99.33
(b) Epoxy\0.5 wt. % CuO	0.5	99.48
(c) Epoxy\1.0 wt. % CuO	1.0	99.75
(d) Epoxy\1.5 wt. % CuO	1.5	100.00
(e) Epoxy\2.0 wt. % CuO	2.0	100.00
(f) Epoxy\2.5 wt. % CuO	2.5	100.00

3.5 *Photoluminescence*

CuO photoluminescence spectroscopy was performed to find the CuO light emission when it is stimulated by light of a specific wavelength. CuO samples can have their electrons stimulated from their ground state to higher energy levels when they are exposed to light. CuO typically has a broad band of photoluminescence centered between 240 and 420 nm, corresponding to the emission of red light. The observed red emission is the result of a photon being released when an excited electron recombines with a hole at an oxygen vacancy shown in Figure 10. Several variables, including the excitation wavelength, temperature, and the presence of defects or impurities in the material, can affect the intensity and structure of the photoluminescence spectrum. The CuO polymer composite spectra revealed many 400–800 nm peaks. Peak shifting is the process wherein the peak location moves toward longer wavelengths as the excitation wavelength increases

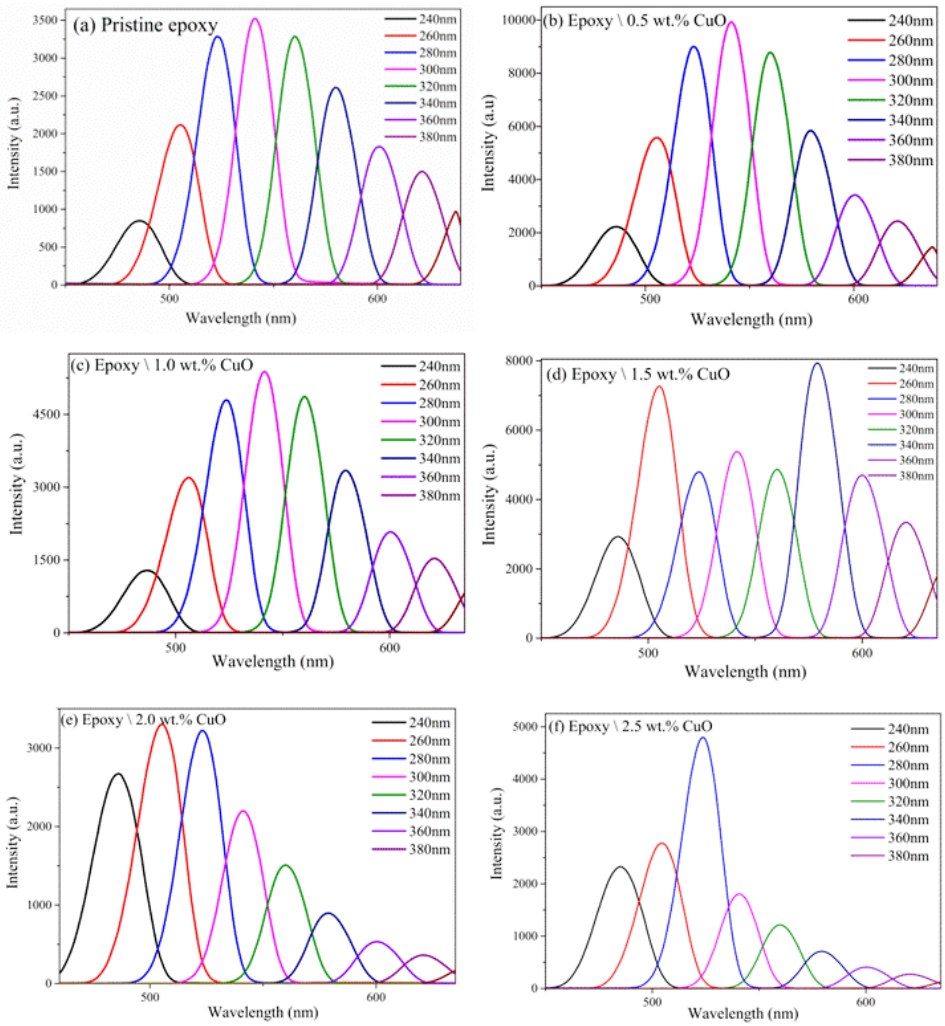

Figure 11: Luminescence spectra of (a) Pristine epoxy, (b) Epoxy\0.5 wt.% CuO, (c) Epoxy\1.0 wt.% CuO, (d) Epoxy\1.5 wt.% CuO, (e) Epoxy\2.0 wt.% CuO, and (f) Epoxy\2.5 wt.% CuO.

shown in Figure 11. The re-absorption of photons by the nanoparticles, which causes a longer path length and a redshift of the photoluminescence peak is caused by the peak shifting [51].

As confirmation that light recombination produces a hole with a single ionized electron in the valence band, the intensity of a single ionized oxygen vacancy gives rise to the red emission peak at 600 nm. The energy transfer between CuO nanoparticles and the polymer composite can be used to explain this property. The PL result leads to the conclusion that red-emitting optoelectronic devices can be designed using the CuO nanoparticles loading polymer composite. It is clear that the intensity increase changes depending on the amount of CuO loaded into the polymer composite [52]. It is worth noticing the incorporation of CuO nanoparticles into epoxy polymer showed an increase in the intensity. This may be the reason that upon irradiation of the sample, more and more electronics are excited to the surface and improved the conducting property of the composite as shown in Figure 11(b)–(f). Hence, these composites find applications in electronics and better thermal qualities for reinforcement.

Polymer nanocomposites have diverse applications in packaging and barrier coatings. By incorporating CuO nanoparticles, these composites can greatly

enhance barrier properties, making them well-suited for protective uses like food packaging. CuO integration elevates polymer films, expanding their capabilities for safeguarding various products.

The future scope of this work could involve further optimization of the CuO nanoparticle content to achieve an ideal balance between enhanced properties and cost-effectiveness. Additionally, exploring the compatibility of these composites with different polymer matrices and investigating their performance under various environmental conditions could open up new avenues of application. Further research into the fundamental mechanisms behind the observed peak shifting and photoluminescence behavior could contribute to the design of tailored luminescent materials. Finally, scalability and manufacturability considerations are essential for transitioning these findings into practical industrial applications [53]–[59].

The SEM analysis revealed that CuO nanoparticles were uniformly distributed within the epoxy, forming spherical particles. The uniform distribution of nanoparticles in epoxy is crucial for improving mechanical properties, making these composites suitable for applications in the aerospace and automobile industries where lightweight, strong materials are essential. TGA results showed minimal mass loss below 250 °C for nano-CuO polymer composites, indicating excellent thermal stability. The thermal stability makes these composites ideal for high-temperature applications, such as components in the aerospace industry or the construction of high-temperature-resistant materials. Photoluminescence exhibited redshifted luminescence spectra. The study suggests that the integration of CuO nanoparticles into epoxy enhances its qualities, with critical influence from CuO loading. The test results demonstrate that the integration of CuO nanoparticles into epoxy polymer composites can yield materials with a wide range of applications, from high-strength aerospace components to thermally stable adhesives. These findings open up opportunities for innovative solutions across multiple industries.

4 Conclusions

In this work, CuO nanoparticles were synthesized through the solution combustion method and subsequently impregnated into an epoxy matrix using ultrasonication for uniform dispersion. The aim was to reinforce epoxy composite properties with CuO. The chosen matrix was Lapox L12 and Hardener K6. Comprehensive material characterization techniques were employed for morphology, elemental composition, phase identification, thermal, and optical properties. SEM images revealed permeable CuO nanoparticles prone to aggregation at higher concentrations. Samples containing 0.5 wt% CuO displayed agglomerated spherical particles. EDX analysis confirmed Cu and O presence in CuO nanoparticles. XRD patterns validated CuO phase formation, with specific peaks at approximately 26.25° in CuO nanofiller-impregnated samples. FTIR spectra demonstrated a distinctive peak at 3713 cm^{-1} denoting OH stretching vibrations. In CuO-impregnated epoxy polymer composites, CuO stretching vibration peak intensity correlated directly with CuO concentration, intensifying from 0.5–2.5 wt.%. TGA analysis for pure CuO showcased no mass loss at 250 °C, retaining 98% mass at 900 °C. With 0.5 wt.% addition, the onset temperature increased. CuO-impregnated epoxy polymer composites (0.5–2.5 wt.%) retained 99–100% mass at 250°C, reflecting improved thermal stability. However, higher CuO content reduced degradation onset temperature. Luminescence spectra for CuO nanoparticles and CuO polymer composites exhibited peaks within the 400–800 nm range. Peak shifting, a phenomenon of peak location transitioning to longer wavelengths with increased excitation wavelength, was observed. This shift results from nanoparticles re-absorbing photons, causing a redshift in the photoluminescence peak. This study underscores the potential of integrating a minute quantity of CuO nanoparticles to fabricate advanced multi-scale polymer composites. It envisions the potential of hybridizing nano- and micro-scale particles in fiber-reinforced polymer matrix materials, offering heightened attributes and capabilities for various applications.

Acknowledgements

The authors acknowledge the Centre for Advanced Materials Technology of M. S. Ramaiah Institute of Technology, Bangalore, Karnataka, India for the necessary characterization facilities used in this study. SEM-EDX characterization was performed at BMS College of Engineering, Bangalore, Karnataka, India.

Author Contributions

G.P.: conceptualization, investigation, methodology, writing an original draft; G.M.M.: research design, data analysis, reviewing, resources, supervision, and editing; N.K.: reviewing and editing, All authors have read and agreed to the published version of the manuscript.

Conflicts of Interest

The authors of this work declare no conflict of interest, and there is no funding organization is involved in this research.

References

[1] I. O. Oladele, T. F. Omotosho, G. S. Ogunwande, and F. A. Owa, "A review on the philosophies for the advancement of polymer-based composites: Past, present and future perspective," *Applied Science and Engineering Progress*, vol. 14, no. 4, pp. 553–579, Oct.–Dec. 2021, doi: 10.14416/j.asep.2021.08.003.

[2] A. D. Printz and D. J. Lipomi, "Competition between deformability and charge transport in semiconducting polymers for flexible and stretchable electronics," *Applied Physics Reviews*, vol. 3, no. 2, Jun. 2016, Art. no. 021302, doi: 10.1063/1.4947428.

[3] A. Hamisu, U. I. Gaya, and A. H. Abdullah, "Bi-template assisted sol-gel synthesis of photocatalytically-active mesoporous anatase TiO_2 nanoparticles," *Applied Science and Engineering Progress*, vol. 14, no. 3, pp. 313–327, 2021, doi: 10.14416/j.asep.2021.04.003.

[4] J. K. Rao, A. Raizada, D. Ganguly, M. Mankad, S. Satayanarayana, and G. M. Madhu, "Investigation of structural and electrical properties of novel CuO–PVA nanocomposite films," *Journal of Materials Science*, vol. 50, no. 21, 2015, doi: 10.1007/s10853-015-9261-0.

[5] B. D. S. Deeraj, K. Joseph, J. S. Jayan, and A. Saritha, "Dynamic mechanical performance of natural fiber reinforced composites: A brief review," *Applied Science and Engineering Progress*, vol. 14, no. 4, pp. 614–623, 2021, doi: 10.14416/j.asep.2021.06.003.

[6] W. Zhao, Y. Jiao, J. Li, L. Wu, A. Xie, and W. Dong, "One-pot synthesis of conjugated microporous polymers loaded with superfine nano-palladium and their micropore-confinement effect on heterogeneously catalytic reduction," *Journal of Catalysis*, vol. 378, pp. 42–50, 2019, doi: 10.1016/j.jcat.2019.07.056.

[7] G. D. Mogosanu, and A. M. Grumezescu, "Natural and synthetic polymers for wounds and burns dressing," *International Journal of Pharmaceutics*, vol. 463, no. 2, pp. 127–136, 2014, doi: 10.1016/j.ijpharm.2013.12.015.

[8] A. Rita, A. Sivakumar, and S. A. M. B. Dhas, "Influence of shock waves on structural and morphological properties of copper oxide NPs for aerospace applications," *Journal of Nanostructure in Chemistry*, vol. 9, pp. 225–230, 2019, doi: 10.1007/s40097-019-00313-0.

[9] C. Srikanth and G. M. Madhu, "Synthesis, characterization and properties evaluation of ZrO_2 and its composites–A review," in *International Conference on Advances in Thermal Systems, Materials and Design Engineering (ATSMDE2017)*, 2017, doi: 10.2139/ssrn.3101419.

[10] M. E. Hoque, A. M. Rayhan, and S. I. Shaily, "Natural fiber-based green composites: Processing, properties and biomedical applications," *Applied Science and Engineering Progress*, vol. 14, no. 4, pp. 689–718, 2021, doi: 10.14416/j.asep.2021.09.005.

[11] A. S. Mukasyan, P. Epstein, and P. Dinka, "Solution combustion synthesis of nanomaterials," *Proceedings of the Combustion Institute*, vol. 31, no. 2, pp. 1789–1795, 2007, doi: 10.1016/j.proci.2006.07.052.

[12] E. Novitskaya, J. P. Kelly, S. Bhaduri, and O. A. Graeve, "A review of solution combustion synthesis: An analysis of parameters controlling powder characteristics," *International Materials Reviews*, vol. 66, no. 3, pp. 188–214, 2020, doi: 10.1080/09506608.2020.1765603.

[13] T. P. Ye, S. F. Liao, Y. Zhang, M. J. Chen, Y. Xiao, X. Y. Liu, and D. Y Wang, "Cu(0) and Cu(II) decorated graphene hybrid on improving fireproof efficiency of intumescent flame-retardant epoxy resins," *Composites Part B: Engineering*, vol. 175, 2019, Art. no. 107189, doi: 10.1016/j.compositesb.2019.107189.

[14] C. Zhang, R. Huang, Y. Wang, Z. Wu, S. Guo, H.

Zhang, and L. Li, "Aminopropyltrimethoxysilane-functionalized boron nitride nanotube based epoxy nanocomposites with simultaneous high thermal conductivity and excellent electrical insulation," *Journal of Materials Chemistry A*, vol. 6, no. 42, pp. 20663–20668, 2018, doi: 10.1039/C8TA07435F.

[15] A. G. Niculescu, C. Chircov, A. C. Bîrcă, and A. M. Grumezescu, "Nanomaterials synthesis through microfluidic methods: An updated overview," *Nanomaterials*, vol. 11, no. 4, 2021, Art. no. 864, doi: 10.3390/nano11040864.

[16] O. Zabihi, M. Ahmadi, T. Abdollahi, S. Nikafshar, and M. Naebe, "Collision-induced activation: Towards industrially scalable approach to graphite nanoplatelets functionalization for superior polymer nanocomposites," *Scientific Reports*, vol. 7, no. 1, 2017, Art. no. 3560, doi: 10.1038/s41598-017-03890-8.

[17] S. J. Kashyap, R. Sankannavar, and G. M. Madhu, "Insights on the various structural, optical and dielectric characteristics of La1-xCaxFeO$_3$ perovskite-type oxides synthesized through solution-combustion technique," *Applied Physics A*, vol. 128, no. 6, Jun. 2022, doi: 10.1007/s00339-022-05628-4.

[18] B. Shaabani, E. Alizadeh-Gheshlaghi, Y. Azizian-Kalandaragh, and A. Khodayari, "Preparation of CuO nanopowders and their catalytic activity in photodegradation of Rhodamine-B," *Advanced Powder Technology*, vol. 25, no. 3, pp. 1043–1052, 2014, doi: 10.1016/j.apt.2014.02.005.

[19] A. M. Kumar, A. Khan, R. Suleiman, M. Qamar, S. Saravanan, and H. Dafalla, "Bifunctional CuO/TiO$_2$ nanocomposite as nanofiller for improved corrosion resistance and antibacterial protection," *Progress in Organic Coatings*, vol. 114, pp. 9–18, Jan. 2018, doi: 10.1016/j.porgcoat.2017.09.013.

[20] M. Puttegowda, H. Pulikkalparambil, and S. M. Rangappa, "Trends and developments in natural fiber composites," *Applied Science and Engineering Progress*, vol. 14, no. 4, pp. 543–552, 2021, doi: 10.14416/j.asep.2021.06.006.

[21] A. Dhandapani, S. Krishnasamy, T. Ungtrakul, S. M. K. Thiagamani, R. Nagarajan, C. Muthukumar, and G. Chinnachamy, "Desirability of tribo-performance of natural based thermoset and thermoplastic composites: A concise review," *Applied Science and Engineering Progress*, vol. 14, no. 4, pp. 606–613, 2021, doi: 10.14416/j.asep.2021.07.001.

[22] K. Setswalo, N. Molaletsa, O. P. Oladijo, E. T. Akinlabi, S. M. Rangappa, and S. Siengchin, "The influence of fiber processing and alkaline treatment on the properties of natural fiber-reinforced composites: A review," *Applied Science and Engineering Progress*, vol. 14, no. 4, pp. 632–650, Oct.–Dec. 2021, doi: 10.14416/j.asep.2021.08.005.

[23] C. Santos, T. Santos, K. Moreira, M. Aquino, and R. F. L. Zillio, "Statistical studyof the influence of fiber content, fiber length and critical length in the mechanical behavior of polymeric composites reinforced with Carica Papaya Fibers (CPFs)," *Applied Science and Engineering Progress*, vol. 14, no. 4, pp. 719–726, 2021, doi: 10.14416/j.asep.2021.07.002.

[24] J. Njuguna and K. Pielichowski, "Polymer nanocomposites for aerospace applications: Properties," *Advanced Engineering Materials*, vol. 5, no. 11, pp. 769–778, 2003, doi: 10.1002/adem.200310101.

[25] J. Njuguna and K. Pielichowski, "Polymer nanocomposites for aerospace applications: Characterization," *Advanced Engineering Materials*, vol. 6, no. 4, pp. 204–210, 2004, doi: 10.1002/adem.200305110.

[26] V. T. Rathod, J. S. Kumar, and A. Jain, "Polymer and ceramic nanocomposites for aerospace applications," *Applied Nanoscience*, vol. 7, no. 8, pp. 519–548, 2017, doi: 10.1007/s13204-017-0592-9.

[27] M. S. Alam and M. A. Chowdhury, "Characterization of epoxy composites reinforced with CaCO$_3$-Al$_2$O$_3$-MgO-TiO$_2$/CuO filler materials," *Alexandria Engineering Journal*, vol. 59, no. 6, pp. 4121–4137, 2020, doi: 10.1016/j.aej.2020.07.017.

[28] M. Asim, M. T. Paridah, M. Chandrasekar, R. M Shahroze, M. Jawaid, M. Nasir, and R. Siakeng, "Thermal stability of natural fibers and their polymer composites," *Iranian Polymer Journal*, vol. 29, no. 7, pp. 625–648, 2020, doi: 10.1007/s13726-020-00824-6.

[29] S. Kharbanda, T. Bhadury, G. Gupta, D. Fuloria, P. R. Pati, V. K. Mishra, and A. Sharma, "Polymer

composites for thermal applications – A review," *Materials Today: Proceedings*, vol. 47, pp. 2839–2845, 2021, doi: 10.1016/j.matpr.2021.03.609.

[30] Z. Barani, A. Mohammadzadeh, A. Geremew, C. Huang, D. Coleman, L. Mangolini, and A. A. Balandin, "Thermal properties of the binary-filler hybrid composites with graphene and copper nanoparticles," *Advanced Functional Materials*, vol. 30, no. 8, 2019, Art. no. 1904008, doi: 10.1002/adfm.201904008.

[31] M. A. V. Anand, K. Saravanakumar, S. Anbazhagan, K. Venkatachalam, and M. H. Wang, "Folic acid functionalized starch encapsulated green synthesized copper oxide nanoparticles for targeted drug delivery in breast cancer therapy," *International Journal of Biological Macromolecules*, vol. 164, pp. 2073–2084, 2020, doi:10.1016/j.ijbiomac.2020.08.03.

[32] B. Ashok, M. Umamahesh, N. Hariram, S. Siengchin, and A. V. Rajulu, "Modification of waste leather trimming with in situ generated silver nanoparticles by one step method," *Applied Science and Engineering Progress*, vol. 14, no. 2, pp. 236–246, 2021, doi: 10.14416/j.asep.2021.01.007.

[33] S. J. Kashyap, R. Sankannavar, and G. M. Madhu, "Hydroxyapatite nanoparticles synthesized with a wide range of Ca/P molar ratios and their structural, optical, and dielectric characterization," *Journal of the Korean Ceramic Society*, vol. 59, pp. 846–858, 2022, doi: 10.1007/s43207-022-00225-w.

[34] F. Gortner, L. Medina, and P. Mitschang, "Influence of Textile Reinforcement on Bending Properties and Impact Strength of SMC-components," *KMUTNB International Journal of Applied Science and Technology*, vol. 8, no. 4, pp. 259–269, 2015, doi: 10.14416/j.ijast.2015.07.005.

[35] V. Tulatorn, S. Ouajai, R. Yeetsorn, and N. Chanunpanich, "Mechanical behavior investigation of UHMWPE composites for pile cushion applications," *KMUTNB International Journal of Applied Science and Technology*, vol. 8, no. 4, pp. 271–282, 2015, doi: 10.14416/j.ijast.2015.08.001.

[36] A. Boontum, J. Phetsom, W. Rodiahwati, K. Kitsubthawee, and T. Kuntothom, "Characterization of diluted-acid pretreatment of water hyacinth," *Applied Science and Engineering Progress*, vol. 12, no. 4, pp. 253–263, Oct.–Dec. 2019, doi: 10.14416/j.asep.2019.09.003.

[37] C. Srikanth, and G. M. Madhu, "Effect of ZTA concentration on structural, thermal, mechanical and dielectric behavior of novel ZTA–PVA nanocomposite films," *SN Applied Sciences*, vol. 2, no. 3, 2020, doi:10.1007/s42452-020-2232-3.

[38] A. Kumar, E. E. Wolf, and A. S. Mukasyan, "Solution combustion synthesis of metal nanopowders: Copper and copper/nickel alloys," *AIChE Journal*, vol. 57, no. 12, pp. 3473–3479. 2011, doi:10.1002/aic.12537.

[39] W. Jansomboon, P. Brikshasri, S. Sarawutanukul, and P. Prapainainar, "Characterization of graphene synthesized by modified hummers and liquid-phase exfoliation method," *Applied Science and Engineering Progress*, vol. 12, no. 1, pp. 14–19, 2019, doi: 10.14416/j.ijast.2018.10.009.

[40] C. Srikanth and G. M. Madhu, "Effect of nano CdO-ZnO content on structural, thermal, optical, mechanical and electrical properties of epoxy composites," *Journal of Metals, Materials, and Minerals*, vol. 33, no. 2, pp. 38–52, Jun. 2023. doi: 10.55713/jmmm.v33i2.1590.

[41] M. Thanasiriruk, P. Saychoo, C. Khajonvittayakul, V. Tongnan, U. W. Hartley, and N. Laosiripojana, "Optimizing operating conditions for Oxidative Coupling Methane (OCM) in the presence of NaCl-MnOx/SiO_2," *Applied Science and Engineering Progress*, vol. 14, no. 3, pp. 477–488, 2021, doi: 10.14416/j.asep.2020.10.001.

[42] S. J. Kashyap, R. Sankannavar, and G.M. Madhu, "Synthesis and characterization of La(Ce, Ba) NiO_3 perovskite-type oxides," *Journal of Superconductivity and Novel Magnetism*, vol. 35, no. 7, pp. 2107–2118, 2022, doi: 10.1007/s10948-022-06219-3.

[43] J. S. Sagar, G. M. Madhu, J. Koteswararao, and P. Dixit, "Studies on thermal and mechanical behavior of nano TiO_2 - epoxy polymer composite," *Communications in Science and Technology*, vol. 7, no. 1, pp. 38–44, 2022, doi: 10.21924/cst.7.1.2022.667.

[44] J. Y. Lambongang and P. Suwanpinij, "Materials characterization techniques for the analyses of components of port fuel injectors," *Applied Science and Engineering Progress*, vol. 13, no. 1,

pp. 48–55, 2020, doi: 10.14416/j.ijast.2018.11.008.
[45] S. Thanomchat, K. Srikulkit, B.Suksut, and A.K. Schlarb, "Morphology and crystallization of polypropylene/microfibrillated cellulose composites," *Applied Science and Engineering Progress*, vol. 7, no. 4, pp. 23–34, 2014, doi: 10.14416/j.ijast.2014.09.002.
[46] N. Salahudeen, "Metakaolinization effect on the thermal and physiochemical propperties of Kankara kaolin," *KMUTNB International Journal of Applied Science and Technology*, vol. 11, no. 2, pp. 127–135, 2018, doi: 10.14416/j.ijast.2018.04.003.
[47] S. Chotisuwan, K. Wannarit, P. Kaewna, S. Kardae, Y. Chaisuksan, and J. Roumcharoen, "Fire-retardant paper based on montmorillonite and oil palm trunk fibres," *Applied Science and Engineering Progress*, vol. 12, no. 4, pp. 277–285, 2019, doi: 10.14416/j.ijast.2018.11.002.
[48] S. J. Kashyap, R. Sankannavar, and G. M. Madhu, "Iron oxide (Fe_2O_3) synthesized via solution-combustion technique with varying fuel-to-oxidizer ratio: FT-IR, XRD, optical and dielectric characterization," *Materials Chemistry and Physics*, vol. 286, 2022, Art. no. 126118, doi: 10.1016/j.matchemphys.2022.126118.
[49] J. Foungchuen, N. Pairin, and C. Phalakornkule, "Impregnation of chitosan onto activated carbon for adsorption selectivity towards CO_2: Biohydrogen purification," *KMUTNB International Journal of Applied Science and Technology*, vol. 9, no. 3, pp. 197–209, 2016, doi: 10.14416/j.ijast.2016.03.003.
[50] C. Srikanth, G. M. Madhu, and S. J. Kashyap, "Enhanced structural, thermal, mechanical and electrical properties of nano ZTA/epoxy composites," *AIMS Materials Science*, vol. 9, no. 2, pp. 214–235, 2022, doi: 10.3934/matersci.2022013.
[51] N. Kottam and S. P. Smrithi, "Luminescent carbon nanodots: Current prospects on synthesis, properties and sensing applications," *Methods and Applications in Fluorescence*, vol. 9, no. 1, Jan. 2021, Art. no. 012001, doi: 10.1088/2050-6120/abc008.
[52] R. Gopalakrishnan and M. Ashokkumar, "Rare earth metals (Ce and Nd) induced modifications on structural, morphological, and photoluminescence properties of CuO nanoparticles and antibacterial application," *Journal of Molecular Structure*, vol. 1244, 2021, Art. no. 131207, doi: 10.1016/j.molstruc.2021.13120.
[53] O. Oladele, T. F. Omotosho, G. S. Ogunwande, and F. A. Owa, "A review on the philosophies for the advancement of polymer-based composites: Past, present and future perspective," *Applied Science and Engineering Progress*, vol. 14, no. 4, pp. 553–579, 2021, doi: 10.14416/j.asep.2021.08.00.
[54] F. Gortner, L. Medina, and P. Mitschang, "Influence of textile reinforcement on bending properties and impact strength of SMC-components," *KMUTNB International Journal of Applied Science and Technology*, vol. 8, no. 4, pp. 259–269, 2015, doi: 10.14416/j.ijast.2015.07.005.
[55] K. Jayappa, V. Kumar, and G. G. Purushotham, "Effect of reinforcements on mechanical properties of nickel alloy hybrid metal matrix composites processed by sand mold technique," *Applied Science and Engineering Progress*, vol. 14, no. 1, pp. 44–51, 2021, doi: 10.14416/j.asep.2020.11.001.
[56] S. Thipperudrappa, A. Hiremath, and B. K. Nagaraj, "Synergistic effect of ZnO and TiO_2 nanoparticles on the thermal stability and mechanical properties of glass fiber-reinforced LY556 epoxy composites," *Polymer Composites*, vol. 42, no. 9, pp. 4831–4844, 2021, doi: 10.1002/pc.26193.
[57] W. H. Kan and L. Chang. "The mechanisms behind the tribological behaviour of polymer matrix composites reinforced with TiO_2 nanoparticles," *Wear*, vol. 474–475, 2021, doi:10.1016/j.wear.2021.203754.
[58] A. Sadooghi and S. J. Hashemi, "Investigating the influence of ZnO, CuO, Al_2O_3 reinforcing nanoparticles on strength and wearing properties of Aluminum matrix nanocomposites produced by powder metallurgy process," *Materials Research Express*, vol. 6, no. 10, 2019, Art. no. 105019, doi: 10.1088/2053-1591/ab3613.
[59] N. W. Khun, H. Zhang, L. H. Lim, and J. L. Yang, "Mechanical and tribological properties of graphene modified epoxy composites," *KMUTNB International Journal of Applied Science and Technology*, vol. 8, no. 2, pp. 101–109, 2015, doi: 10.14416/j.ijast.2015.04.001.